ACS OMEGA

http://pubs.acs.org/journal/acsodf

Article

Studies on Evaluation of the Thermal Conductivity of Alumina Titania Hybrid Suspension Nanofluids for Enhanced Heat Transfer Applications

Atul Bhattad, B. Nageswara Rao, Vinay Atgur, Nagaraj R. Banapurmath, Ashok M. Sajjan,* Chandramouli Vadlamudi, Sanjay Krishnappa, T. M. Yunus Khan, and Narasimha H. Ayachit

Cite This: *ACS Omega* 2023, 8, 24176−24184

Read Online

ACCESS | Metrics & More | Article Recommendations

ABSTRACT: Extensive investigations were made and empirical relations were proposed for the thermal conductivity of mono-nanofluids. The effect of concentration, diameter, and thermal properties of participating nanoparticles is missing in the majority of existing thermal conductivity models. An attempt is made to propose a model that considers the influence of such missing parameters on the thermal conductivity of hybrid nanofluids. Al_2O_3−TiO_2 hybrid nanofluids have a 0.1% particle volume concentration prepared with distinct particle volume ratios (k − 1:6 − k, k = 1 to 6) in DI water. The samples were characterized, and the size and shape of the nanoparticles were verified. Also, the influence of varying particle volume ratios and the fluid temperature (varying from 283 to 308 K) were examined. 2.4 and 2.1% enhancements were observed in the thermal conductivity of alumina (5:0) and titania (0:5) nanofluids (having 0.1% volume concentration), respectively. Due to the low thermal conductivity of titania nanoparticles, the conductivity of the hybrid solution is above that of titania and below that of alumina nanofluids. An empirical relation for the thermal conductivity of hybrid nanofluids is established and validated considering the individual particle size, volume ratio, and thermal conductivity of particles.

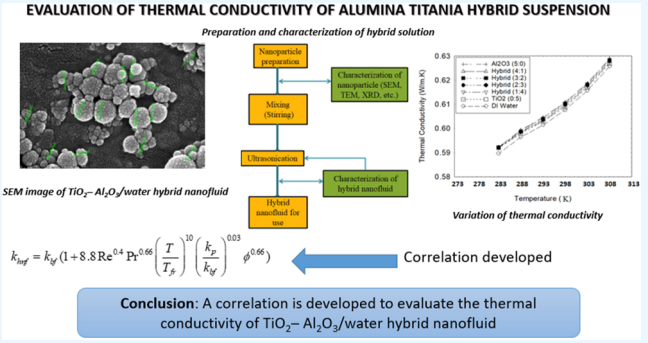

1. INTRODUCTION

The low thermal conductivity of heat transfer fluids affected the performance of heat exchangers. Heat transfer through conduction depends on thermal conductivity, which is further related to the Nusselt number.

1.1. Mono-Nanofluids. The fluids dispersed with nanoparticles (known as nanofluids) enhance heat transfer due to high thermal conductivity. By suspending nanoparticles in base fluids,[1] nanofluids are prepared. The two-step method creates a stable solution by dispersing the fluids with powdered nanoparticles.[2] Such mixtures change the thermophysical properties (viz., viscosity, density, and thermal conductivity). Heat exchangers,[3] thermosyphons,[4] absorption refrigeration systems,[5] and solar energy[6] use nanofluids. The temperature oscillation method,[7] transient hot-wire method,[8] and 3-ω method[9] are used for measuring the thermal conductivity of nanofluids. Empirical relations for the thermal conductivity of nanofluids rely on the measured data. Unjustified assumptions in models bring controversy.[10−13]

1.2. Hybrid Nanofluids. Hybrid nanofluids[14] were introduced for improving the thermal conductivity.[15,16] Qi et al.[17] and Das et al.[18] examined the stability, thermal properties, and convective heat transfer performance of the TiO_2−water nanofluid. Alkasmoul et al.[19] have specified heat flux to examine TiO_2−water and Al_2O_3−water nanofluids in a horizontal tube for cooling. Khaleduzzaman et al.[20] performed energetic and exergetic analysis using CuO−water and TiO_2−water nanofluids for cooling electronic appliances. The CuO−water nanofluids provided appreciable energy efficiency. Senthilkumar et al.[21] and Maddah et al.[22] performed heat transfer analysis in a heat exchanger (HEX) using Al_2O_3/TiO_2 hybrid nanofluids and observed enhancement in heat transfer characteristics as well as the effectiveness of heat exchangers. Hamid et al.[23,24] witnessed 16 and 35.32% improvements in thermal conductivity and the heat transfer rate, respectively, by TiO_2/SiO_2 hybrid nanofluids. Several investigators[25−31] had proposed thermal conductivity models for water-based hybrid nanofluids. They considered separately the influence of

Received: November 23, 2022
Accepted: June 14, 2023
Published: June 27, 2023

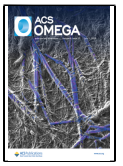

thermal properties of the base fluid and nanoparticles, individual particle size, and concentration.

1.3. Investigations on the Stability of Nanofluids. Das et al.[32] examined a thermal medium (which is synthesized through the mixing of the methyl triphenyl phosphonium bromide salt with ethylene glycol at a 1:4 molar ratio). The shape and morphology of the MWCNTs were ascertained utilizing field emission scanning electron microscopy (FESEM) and field emission transmission electron microscopy (FETEM). The stability of nanofluids was examined by ζ potential measurements in addition to the visual observations. The stability of nanofluids can be improved by preparing the nanofluids through an expensive and complex single-step method.[33]

In fact, the simple two-step method is being adopted in the preparation of nanofluids by the majority of researchers (95%), and it does not require any sophisticated apparatus. For better dispersion of nanoparticles, 3−10 h of sonication time is required.[34] Amin et al.[35] reviewed the characteristics of hybrid (organic and synthetic) nanofluids. Malika and Sonawane[36] followed a two-step method while making CuO−ZnO/water-based hybrid nanofluids (of 0.01 vol % at various mixed ratios). Sahoo and Kumar,[37] Ramadhan et al.,[38] and Wcislik[39] performed the ζ potential analysis for investigating the stability of mono, binary, and trihybrid nanofluids. Afshari et al.[40] made a review and highlighted the technologies to improve the stability of nanofluids. Arora and Gupta[41] have discussed the stability and enhancement techniques. Zainon and Azmi[42] discussed the stability of nanofluids highlighting the sonication process, pH modification, and the surfactants. Bumataria et al.[43] reviewed heat pipe technology with mono- and hybrid nanofluids. The addition of dispersants and sonication are notable methods of enhancing nanofluid stability.[44]

1.4. Motivation. There is a need for a reliable thermal conductivity model for Al_2O_3−TiO_2−water hybrid nanofluids. The model should take care of the thermal properties of particles and the base fluid, size, and volume fraction of nanoparticles. Taguchi's design of experiments was performed by preparing Al_2O_3−TiO_2 hybrid nanofluids. The outline of this article is as follows: Section 2 describes the characteristics of hybrid nanofluids. Section 3 highlights Taguchi's DOE (design of experiments) and OA (orthogonal array) to specify the optimal concentration of nanoparticles to achieve maximum thermal conductivity. Section 4 is devoted to the validation of the developed empirical relations for the thermal conductivity of mono- and hybrid nanofluids.

2. PREPARATION AND CHARACTERIZATION OF HYBRID NANOFLUIDS

Al_2O_3−TiO_2 hybrid nanofluids having 0.1% particle volume concentration with different particle volume ratios were prepared with distinct particle volume ratios (k − 1:6 − k,k = 1 to 6) in DI water. Details of making the hybrid nanofluids and their characterization are as follows.

2.1. Preparation of Al_2O_3−TiO_2 Hybrid Nanofluids. One-step and two-step methods were followed in the synthesis of nanofluids. In the one-step method, the preparation of nanofluids is done by directly dispersing the nanoparticles in the base fluid, and they exhibit superior stability properties. However, the one-step method is difficult and expensive to prepare nanofluids compared to the two-step method. Due to simplicity, most researchers (95%) use the two-step method while making nanofluids.

In this study, nanoparticles were purchased from Gyan Scientific Institute, Varanasi, India. The two-step method is used to prepare the hybrid suspension. The average size of commercial alumina and titania nanoparticles is 45 and 20 nm, respectively. The molecular weights of alumina and titania nanoparticles are 101.96 and 79.85, respectively. The measured quantity of Al_2O_3 and TiO_2 nanoparticles were mixed with a stirrer in DI water for 1 h, followed by ultrasonication at 40 °C for 3 h to prevent sedimentation. The solution was sonicated using an ultrasonicator (Labman Scientific Instruments, India 40 kHz, 10 liter capacity, with a digital temperature controller and timer). A surfactant (Span-80) was used to prevent particle deposition. TiO_2−Al_2O_3 hybrid nanofluids were prepared in distinct ratios (k − 1:6 − k, k = 1 to 6) with 0.1 vol %. Equation 1 gives the volume fractions of the nanoparticles in the fluid.

$$\phi = \frac{\left\{\left(\frac{m}{\rho}\right)_{p1} + \left(\frac{m}{\rho}\right)_{p2}\right\}}{\left\{\left(\frac{m}{\rho}\right)_{p1} + \left(\frac{m}{\rho}\right)_{p2} + \left(\frac{m}{\rho}\right)_{bf}\right\}} \quad (1)$$

Here, ρ (kg/m^3) is the density, ϕ is the solid volume fraction, and m is the mass (kg).

2.2. Characterization of Al_2O_3−TiO_2 Hybrid Nanofluids. Various techniques used to characterize nanofluids include SEM, TEM, FTIR, and XRD.[32] A scanning electron microscope and transmission electron microscope were used to measure the average size of Al_2O_3 and TiO_2 nanoparticles as 45 and 20 nm, respectively, and by Image software, and the small ones in Figure 1 (Bhattad et al.[45]) represent TiO_2 nanoparticles, and the larger ones Al_2O_3 nanoparticles. XRD was applied to determine the crystal structure. In XRD, an object is irradiated with incoming X-rays, and then the intensity and scattering angle of the X-rays emanating from the object are measured. The XRD results of Al_2O_3 and TiO_2 nanoparticles are shown in Figure 2. Using an X-ray

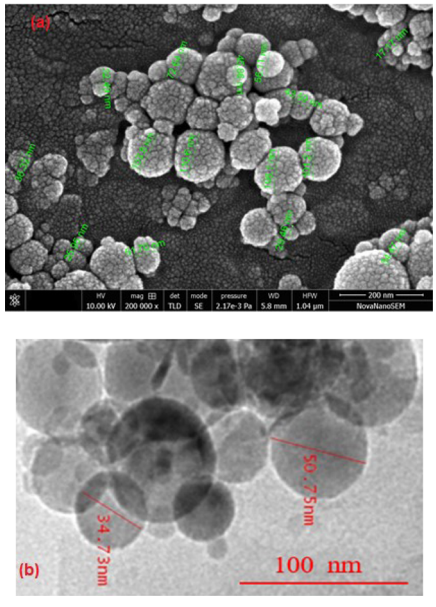

Figure 1. (a) SEM image of the Al_2O_3−TiO_2/water hybrid nanofluid.[45] (b) TEM image of the Al_2O_3−TiO_2/water hybrid nanofluid.[45]

https://doi.org/10.1021/acsomega.2c07513
ACS Omega 2023, 8, 24176−24184

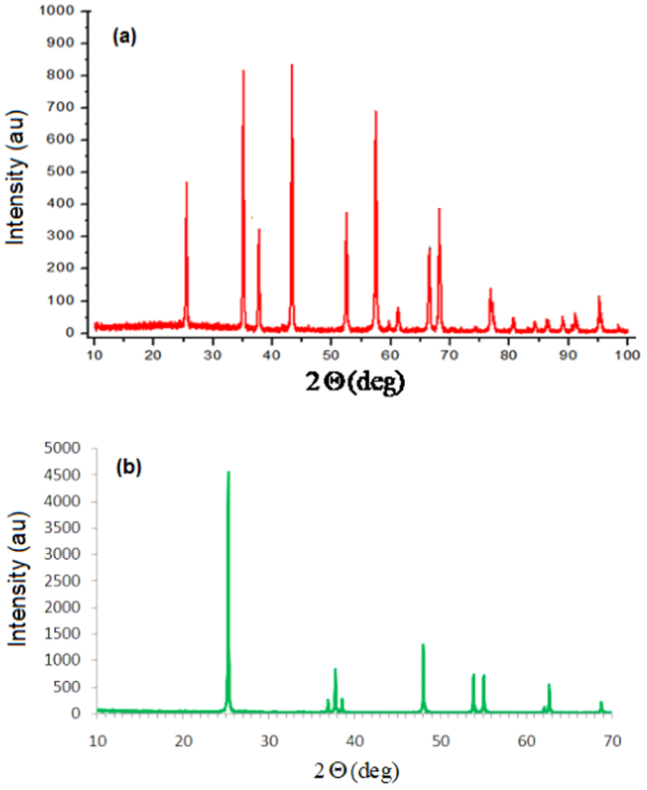

Figure 2. (a) XRD image of Al_2O_3 nanoparticles. (b) XRD image of TiO_2 nanoparticles.

diffractometer (Model Bruker D8, UK) with Cu-Ka radiation, the measured crystal size is 20 nm for titania nanoparticles at a 10−70° angle classified according to the JCPDS No. 21272 standard. The main peak was converted using the Debye−Scherrer formula. Similarly, XRD analysis of Al_2O_3 nanoparticles at a 10−100° angle, according to the JCPDS No. 0100173 standard classification, shows that the crystal size is 45 nm. Al_2O_3 and TiO_2 nanoparticles are spherical (whose shape factor is 1).

Various methods are used to improve the stability of nanofluids.[39] The ζ potential refers to the electrostatic repulsion force between the primary fluid and nanoparticles. The stability of the hybrid nanofluid depends on the magnitude of the repulsion force. For a stable hybrid nanofluid, the ζ potential value lies in a range of 30−60 mV. Xu et al.[46] represented the ζ potential value of 42.6 and 40.8 mV for the highly stable 25:75 (Al_2O_3/TiO_2) hybrid nanofluid and TiO_2 nanofluid, respectively. Hence, for the present study, the ζ potential will be above 30 mV and below 60 mV. The value of the ζ potential decreases with the increase in concentration, which may lead to the suspension of nanoparticles after a long time. The homogeneity of the solution was verified from samples at distinct locations of the beaker. The stability of the synthesized hybrid nanofluid has been analyzed by the concept of isoelectric point (IEP) and the conventional photography method. Sedimentation photography is the simplest and most qualitative method to check the stability of nanofluids visually. From this, the sedimentation of dispersed nanoparticles can be observed with the naked eye. This method also has limitations as it cannot be used for partial sedimentation and higher concentration nanofluids. But in the present investigation, a lower concentration (0.1 vol %) is considered, so this method is reliable for checking the stability. The pH values of the samples fall within 5.66 and 5.73, which is not in the scope of the nanoparticles' isoelectric points due to their repulsive force among the nanoparticles.[22] Stability tests were conducted by taking pictures of the test tube, as shown in Figure 3 (Bhattad et al.[45]), and no sedimentation was observed during the 7-day investigation.

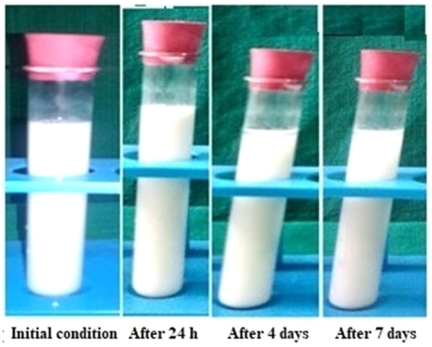

Figure 3. Stability analysis of a sample showing no sedimentation for 7 days.

2.3. Measurement of Thermal Conductivity. The thermal conductivity of Al_2O_3−TiO_2/water hybrid nanofluids was measured with a hot disk thermal constant analyzer (see Figure 4), which works on the transient plane source

Figure 4. Hot disk thermal constant analyzer.[45]

technique. The sensors contain a nickel foil sandwiched between layers of Kapton film. The nickel foil forms a spiral pattern having a 3.189 mm radius. While passing the heating power, spherical waves were generated through the probe end and traveled through the sample. The hot disk measures the thermal conductivity with an accuracy of ± 1.5% under a constant heating rate from the frequency of the temperature rise of the measuring probe. Tests were repeated several times to confirm the measurement accuracy. Table 1 presents the thermophysical properties of DI water (base fluid).

3. TAGUCHI DESIGN OF EXPERIMENTS FOR OPTIMAL SOLUTION

For any new physical phenomenon, it is necessary to observe the phenomenon through experiments before the development of mathematical models. The number of process parameters

Table 1. Thermophysical Properties of DI Water

T (K)	k_{bf} (W/m·K)	ρ_{bf} (kg/m^3)	μ_{bf} (mPa·s)	Pr_{bf}
283	0.582	997.8	0.955	6.77
288	0.589	996.8	0.870	6.10
293	0.596	996.0	0.815	5.66
298	0.601	994.7	0.749	5.16
303	0.607	993.7	0.690	4.69
308	0.614	992.7	0.629	4.22

https://doi.org/10.1021/acsomega.2c07513
ACS Omega 2023, 8, 24176−24184

(n_p) and assigned levels to each parameter (n_l) require n_l^{nP} experiments. The task is involved by increasing n_p and n_l. By performing a few experiments as per Taguchi's orthogonal array,[47] it is possible to generate the data for the full factorial design of experiments. Several investigators adopted Taguchi's design of experiments utilizing Minitab as a computational tool. The modified Taguchi approach[48−51] provides the generation of the complete information with a few experiments, the expected range of performance indicators, and also introduces a simple multiobjective optimization procedure.

In the present study, experiments were performed to examine the influence of varying particle volumetric ratios as well as the fluid temperature on the thermal conductivity (k_{nf}) of an Al_2O_3−TiO_2 hybrid suspension in DI water. ϕ_1 and ϕ_2 are assumed as the Al_2O_3 particle volumetric concentration and the TiO_2 particle volumetric concentration, respectively. T is represented as the fluid temperature. ϕ_1 and ϕ_2 vary within 0.1% volumetric concentration of the hybrid suspension (i.e., $\phi_1 + \phi_2 = 0.1\%$), which indicates the linear dependency of ϕ_1 and ϕ_2. Taguchi's design of the experiment is described to identify the optimal proportion of the concentration of nanoparticles to achieve maximum thermal conductivity. It helps to generate the data for the full factorial design of experiments within the specified range of the parameters. It reduces the number of experiments to be conducted and provides the optimal solution. Taguchi's L_9OA is chosen for 3 process parameters ($n_p = 3$) such as ϕ_1, ϕ_2, and T with 3 levels ($n_l = 3$) using the formula[33]

$$N_{Taguchi} = 1 + n_p \times (n_l - 1) \quad (2)$$

Equation 2 gives the minimum number of experiments, $N_{Taguchi} = 7$, whereas, for all combinations, 27 tests (i.e., $n_l^{n_p} = 3^3$) are to be conducted. In the present study, only 9 test data are considered to obtain the optimal solution for thermal conductivity.

For the linear dependency of ϕ_1 and ϕ_2, ϕ_1 is considered (whereas, $\phi_2 = 0.1 - \phi_1$) and T is the second process parameter. Table 2 presents test data of k_{nf}. For the present case of $N_{Taguchi} = 9$ and $n_l = 3$, eq 2 gives $n_p = 4$. From the literature,[48−51] fictitious parameters (F_1 and F_2) are introduced in Table 2. ANOVA is performed and the results are given in Table 3. It is noted that T has the maximum effect on k_{nf} with a 99.6% contribution. The total % contribution of ϕ_1, T, F_1, and F_2 for k_{nf} is 100. Hence, the % contribution of the fictitious parameters F_1 and F_2 is nothing but the 0.1% error.

Process designer prefers to have a range of estimates for k_{nf} while conducting repeated tests. Following the additive law,[47] $\hat{k}_{nf}$ is estimated for the levels of the process parameters from

$$\hat{k}_{nf} = \bar{k}_{nf}^{(g)} + \sum_{i=1}^{n_p} (\bar{k}_{nf}^{(i)} - \bar{k}_{nf}^{(g)}) = \sum_{i=1}^{n_p} \bar{k}_{nf}^{(i)} - (n_p - 1)\bar{k}_{nf}^{(g)} \quad (3)$$

Here, $\bar{k}_{nf}^{(g)}$ is the grand mean of k_{nf} in test runs, and $\bar{k}_{nf}^{(i)}$ is the mean value of k_{nf} in ANOVA Table 3 for the level of process parameters (i). The superscript, i = 1,2,3, and 4 corresponds to ϕ_1, T, F_1, and F_2, respectively. The estimates of k_{nf} in Table 4 for the 9 test runs of Taguchi's L_9 OA are comparable with test data. $n_p = 2$ and $n_p = 4$ in eq 3 give estimates of k_{nf} without and with fictitious parameters (F_1 and F_2), respectively. The estimates with fictitious parameters match exactly with the test data. Considering only the levels of the minimum and maximum mean values of k_{nf} for F_1 and F_2, the range of estimates arrives from eq 3. For the levels of ϕ_1 and T, corrections to k_{nf} estimates are −0.0006 and 0.0005, respectively. Test data in Table 4 are within the range of k_{nf} estimates.

Table 2. Thermal Conductivity of Hybrid Nanofluids for the Assigned Process Parameters, viz., Al_2O_3 Particle Volume Concentration (%), ϕ_1 with the TiO_2 Particle Volume Concentration (%), $\phi_2 = 0.1 - \phi_1$, and Temperature (T)

(a) assignment levels

process parameters	notation	level-1	level-2	level-3
Al_2O_3 particle volumetric concentration (%)	ϕ_1	0	0.04	0.1
temperature (K)	T	283	293	303
fictitious-1	F_1	f_{11}	f_{12}	f_{13}
fictitious-2	F_2	f_{21}	f_{22}	f_{23}

(b) thermal conductivity (k_{nf})

	levels of process parameters				
test run	ϕ_1	T	F_1	F_2	thermal conductivity, k_{nf} (W/m·K)
1	1	1	1	1	0.591
2	1	2	2	2	0.602
3	1	3	3	3	0.616
4	2	1	2	3	0.592
5	2	2	3	1	0.603
6	2	3	1	2	0.617
7	3	1	3	2	0.592
8	3	2	1	3	0.604
9	3	3	2	1	0.618
grand mean					0.604

Table 3. ANOVA Results on Thermal Conductivity, k_{nf} (W/m·K)

process parameters	1-Mean	2-Mean	3-Mean	sum of squares	% contribution
ϕ_1	0.603	0.604	0.605	2.829×10^{-6}	0.3
T	0.592	0.603	0.617	1.002×10^{-3}	99.6
F_1	0.604	0.604	0.604	5.756×10^{-7}	0.1
F_2	0.604	0.604	0.604	3.289×10^{-7}	0.0

Considering the mean values in ANOVA Table 3 for k_{nf}, the empirical relation developed in terms of process parameters (ϕ_1 and T) is

$$k_{nf} = 0.6036 + 0.0007\xi_1 + 0.0001\xi_1^2 + 0.0129\xi_2 + 0.0013\xi_2^2 \quad (4)$$

Here, $\xi_1 = \frac{1}{3}(25\varphi_1 - 1)(3 - 10\varphi_1)$; and $\xi_2 = \frac{1}{10}(T - 293)$. The lower bound estimates of k_{nf} are obtained by applying correction −0.0006 in eq 4, whereas the upper bound estimates are obtained by applying correction 0.0005 in eq 4. From ANOVA Table 3, a set of process parameters $\phi_{1_3}T_3$ (in which subscripts denote the level of the parameter) are identified for maximum k_{nf}. The optimal process parameters are ϕ_1 = 0.1% and T = 303 K for which eq 4 gives k_{nf} = 0.618W/m·K, which is exactly matching with measured data. This corresponds to the case of 0.1 vol % of Al_2O_3 nanoparticles mixed with DI water, which yields high thermal conductivity. The present result and the result obtained by the Taguchi method were compared, which is displayed in Figure 5.

https://doi.org/10.1021/acsomega.2c07513
ACS Omega 2023, 8, 24176−24184

Table 4. Estimates of the Thermal Conductivity, k_{nf} (W/m·K), and Comparison with Test Data

	level parameters					estimate eq 3			expected range	
test run	ϕ_1	T	F_1	F_2	test	n_p = 2	R.E. (%)	n_p = 4	lower bound	upper bound
1	1	1	1	1	0.591	0.591	0.08	0.591	0.590	0.592
2	1	2	2	2	0.602	0.603	−0.02	0.602	0.602	0.603
3	1	3	3	3	0.616	0.617	−0.05	0.616	0.616	0.617
4	2	1	2	3	0.592	0.592	0.02	0.592	0.591	0.592
5	2	2	3	1	0.603	0.603	−0.02	0.603	0.603	0.604
6	2	3	1	2	0.617	0.617	0.00	0.617	0.617	0.618
7	3	1	3	2	0.592	0.592	−0.10	0.592	0.592	0.593
8	3	2	1	3	0.604	0.604	0.05	0.604	0.603	0.604
9	3	3	2	1	0.618	0.618	0.05	0.618	0.618	0.619

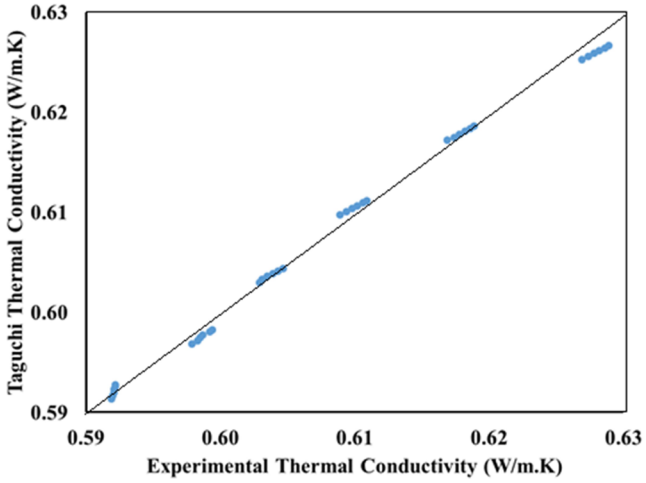

Figure 5. Comparison of test data with Taguchi method results.

4. RESULTS AND DISCUSSION

In this section, the developed empirical relations are presented for mono-nanofluids followed by hybrid nanofluids. The results obtained are discussed in the upcoming sections.

4.1. Mono-Nanofluids. Several empirical relations exist for the nanofluid thermal conductivity in terms of the nanoparticle concentration (ϕ), the thermal conductivity of nanoparticles (k_p), and the base fluid (k_{bf}).[52−55] A few of the frequently used empirical relations (Corcione,[54] Maxwell, Bruggeman et al.,[55] and Hamilton and Crosser[55]) are presented below.

Bruggeman et al.[55]

$$\frac{\phi(k_p - k_{nf})}{(k_p + 2k_{nf})} + (1-\phi)\frac{(k_{bf} - k_{nf})}{k_{bf} + 2k_{nf}} = 0 \quad (5)$$

Maxwell[55]

$$k_{nf} = \frac{k_{bf}(k_p + 2k_{bf} + 2\phi(k_p - k_{bf}))}{(k_p + 2k_{bf} - \phi(k_p - k_{bf}))} \quad (6)$$

Hamilton and Crosser[55]

$$k_{nf} = \frac{k_{bf}(k_p + (n-1)k_{bf} + (n-1)\phi(k_p - k_{bf}))}{(k_p + (n-1)k_{bf} - \phi(k_p - k_{bf}))} \quad (7)$$

Here, the shape factor, n = 3 for a spherical shape.

Corcione[54]

$$k_{hnf} = k_{bf}\left\{1 + 4.4Re^{0.4}Pr^{0.66}\left(\frac{T}{T_{fr}}\right)^{10}\left(\frac{k_p}{k_{bf}}\right)^{0.03}\phi^{0.66}\right\} \quad (8)$$

Here, the reference temperature, T_{fr} = 284 K; Reynolds number, $Re = \frac{2\rho_{bf}k_BT}{\pi d_p \mu_{bf}^2}$; μ_{bf} = fluid viscosity; ρ_{bf} = density of the fluid; d_p = particle diameter; k_p and k_{bf} are the thermal conductivity of the particle and base fluid; Pr = Prandtl number; the Boltzmann constant, $k_B = 1.3807 \times 10^{-23}$; and ϕ = particle concentration.

The thermal conductivity of hybrid nanofluid samples was evaluated experimentally and an accurate empirical relation was modeled through nonlinear regression. Test results of alumina and titania nanofluids are compared using eqs 5−8. It can be seen from Table 5 that the experimental data deviated by 1.2% for Corcione[54] (eq 8). However, the results obtained from eqs 5 to 7 are also comparable with measured data. At low particle concentrations, estimates from eqs 5 to 8 match well. Such a trend is not noticed in the case of high concentrations. Equation 8 is modified to eq 9 and found good comparison with the test data of Tiwari et al.[55] (see Table 6). The test data of Tiwari et al.[55] at 323 K at different particle concentrations and the estimates from empirical relations 5 to 9 are in Table 7.

Table 5. Thermal Conductivity of Al_2O_3 and TiO_2 Nanofluids (0.1 vol %) with Temperature and Comparison with Existing Empirical Relations 5−8

	Al_2O_3 thermal conductivity (W/m·K)					TiO_2 thermal conductivity (W/m·K)				
T (K)	Exp	eq 5	eq 8	eq 7	eq 6	exp	eq 5	eq 8	eq 7	eq 6
283	0.592	0.584	0.584	0.584	0.584	0.591	0.583	0.583	0.583	0.583
288	0.599	0.591	0.591	0.591	0.591	0.597	0.591	0.591	0.591	0.591
293	0.604	0.598	0.599	0.598	0.598	0.602	0.597	0.598	0.597	0.597
298	0.610	0.603	0.604	0.603	0.603	0.608	0.602	0.603	0.602	0.602
303	0.618	0.609	0.611	0.609	0.609	0.616	0.609	0.610	0.609	0.609
308	0.628	0.615	0.618	0.615	0.615	0.626	0.615	0.617	0.615	0.615

https://doi.org/10.1021/acsomega.2c07513
ACS Omega 2023, 8, 24176−24184

Table 6. Thermal Conductivity of Al_2O_3 and TiO_2 nanofluids (0.1 vol %) with Temperature and Comparison with the Developed Empirical Relations 9

	Al_2O_3 thermal conductivity (W/m·K)		TiO_2 thermal conductivity (W/m·K)	
T (K)	exp	eq 9	exp	eq 9
283	0.592	0.585	0.591	0.585
288	0.599	0.593	0.597	0.592
293	0.604	0.601	0.602	0.600
298	0.610	0.607	0.608	0.606
303	0.618	0.615	0.616	0.613
308	0.628	0.623	0.626	0.620

$$k_{hnf} = k_{bf}\left\{1 + 8.8Re^{0.4}Pr^{0.66}\left(\frac{T}{T_{fr}}\right)^{10}\left(\frac{k_p}{k_{bf}}\right)^{0.03}\phi^{0.66}\right\} \quad (9)$$

Table 7. Thermal Conductivity Data of Al_2O_3 Nanofluids at 323 K for Various Concentrations

concentration	K Tiwari[55]	eq 5	eq 9	eq 7	eq 6
0.005	0.688	0.648	0.695	0.648	0.648
0.01	0.723	0.658	0.727	0.658	0.658
0.015	0.748	0.668	0.754	0.667	0.667
0.02	0.773	0.678	0.778	0.676	0.676
0.025	0.799	0.688	0.800	0.686	0.686
0.03	0.817	0.699	0.821	0.696	0.696
0.035	0.840	0.710	0.840	0.705	0.705
0.04	0.859	0.721	0.859	0.715	0.715
0.045	0.877	0.733	0.877	0.725	0.725
0.05	0.896	0.745	0.894	0.735	0.735
0.055	0.912	0.758	0.910	0.745	0.745
0.06	0.928	0.771	0.926	0.756	0.756

At high concentrations, the estimates of eq 9 are close to the test data.[55] Equation 9 incorporates the size of the nanoparticles. From Figure 6, the thermal conductivity of nanofluids

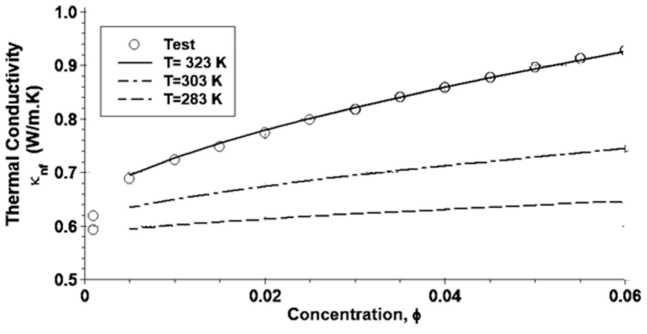

Figure 6. Thermal conductivity of the alumina nanofluid at different temperatures and concentrations.

estimated by the modified Corcione formula (eq 9) increases with temperature as well as particle concentration. Also, the existing test data are in line with eq 9.

4.2. Hybrid Nanofluids. The measured thermal conductivity of nanofluids with temperature is presented in Table 8 and Figure 7. From Table 8, the thermal conductivity of hybrid nanofluids is high compared to that of the base fluid. It is a minimum for 100% titania nanofluids and a maximum for 100% alumina nanofluids. This is mainly due to the low

Table 8. Thermal Conductivity Data of Various Fluids at Different Temperatures and Particle Ratios

	283 K	288 K	293 K	288 K	303 K	308 K
DI water	0.589	0.596	0.601	0.607	0.615	0.625
TiO_2 (0:5)	0.591	0.597	0.602	0.608	0.616	0.626
hybrid (1:4)	0.592	0.598	0.603	0.609	0.617	0.627
hybrid (2:3)	0.592	0.598	0.603	0.609	0.617	0.627
hybrid (3:2)	0.592	0.598	0.603	0.610	0.618	0.628
hybrid (4:1)	0.592	0.599	0.604	0.610	0.618	0.628
Al_2O_3 (5:0)	0.592	0.600	0.605	0.611	0.619	0.629

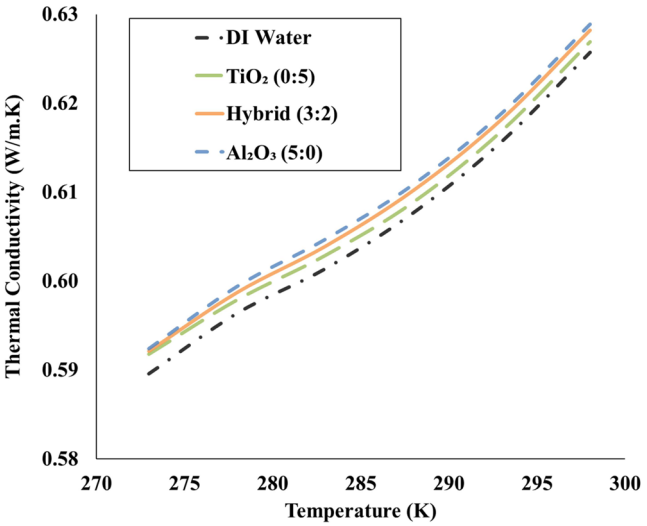

Figure 7. Variation of thermal conductivity for different temperatures.

thermal conductivity of titania particles and the high thermal conductivity of alumina particles. The thermal conductivity of the solution increases with the volume fraction of alumina in the solution. A 0.5% enhancement in thermal conductivity was observed for the Al_2O_3 (5:0) hybrid nanofluids (0.1 vol %). From Figure 7, the thermal conductivity increases with the temperature and the enrichment at a low fluid temperature is relatively small, whereas the improvement of thermal conductivity is significant with an intensification in temperature. The thermal conductivity was found to be a growing function of the particle volume ratio for a given temperature. The particle volume ratio is the affecting parameter for thermophysical properties of nanofluids.

The solid nanoparticle volume ratio and temperature are vital parameters in most of the existing relations for the thermal conductivity of nanofluids. The test results for alumina nanofluids and titania nanofluids are compared with existing empirical relations and found that the empirical relation of thermal conductivity proposed by Corcione[54] provides satisfactory results with a small modification in the coefficient. An attempt is made here for proposing a relation for the thermal conductivity of hybrid nanofluids. In this regard, test results of hybrid nanofluids are compared with existing empirical relations 10 to 13. Figure 8 shows the comparison of empirical and measured thermal conductivity at different temperatures and volume concentrations.

Takabi and Salehi[27]

https://doi.org/10.1021/acsomega.2c07513
ACS Omega 2023, 8, 24176−24184

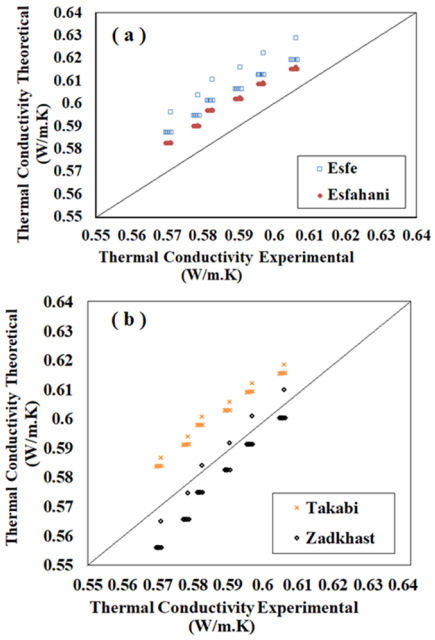

Figure 8. Comparison of measured thermal conductivity of hybrid nanofluids and estimates using empirical relations (a) Hemmat Esfe[29] and Esfahani;[31] and (b) Takabi[27] and Zadkhast.[30]

$$\frac{k_{nf}}{k_{bf}} = \frac{\frac{\phi_1 k_1 + \phi_2 k_2}{\phi} + 2(1-\phi)k_{bf} + 2(\phi_1 k_1 + \phi_2 k_2)}{\frac{\phi_1 k_1 + \phi_2 k_2}{\phi} + 2(1+\phi)k_{bf} - 2(\phi_1 k_1 + \phi_2 k_2)} \quad (10)$$

Hemmat Esfe et al.[29]

$$\frac{k_{nf}}{k_{bf}} = [0.1747 \times 10^5 + \phi]/[0.1747 \times 10^5 - 0.1498 \times 10^6 \phi + 0.1117 \times 10^7 \phi^2 + 0.1997 \times 10^8 \phi^3] \quad (11)$$

Zadkhast et al.[30]

$$\frac{k_{nf}}{k_{bf}} = 0.907 \exp(0.36\phi^{0.3111} + 0.000956T) \quad (12)$$

Esfahani et al.[31]

$$\frac{k_{nf}}{k_{bf}} = 1 + 0.0008794\, \phi^{0.5899} T^{1.345} \quad (13)$$

Estimates from empirical relations 10 to 13 are not matching with test data. There is a need to develop empirical relations for the thermal conductivity of TiO_2−Al_2O_3/water hybrid nanofluids that depend on individual particle concentration, particle diameter, particle thermal conductivity, the thermal conductivity of the base fluid, and temperature of the solution. The Corcione[54] empirical relation modified for hybrid nanofluids is

$$k_{hnf} = k_{bf}\left\{1 + 8.8Re^{0.4}Pr^{0.66}\left(\frac{T}{T_{fr}}\right)^{10}\left(\frac{k_p}{k_{bf}}\right)^{0.03}\phi^{0.66}\right\} \quad (14)$$

Here, T is the working temperature (K); T_{fr} is the reference temperature (K); $k_p = \frac{\phi k_{p1} k_{p2}}{\phi_1 k_{p2} + \phi_2 k_{p1}}$ and $\phi = \phi_1 + \phi_2$; Pr is the Prandtl number; $Re = Re = \frac{\rho_{bf} k_B T}{\pi r_p \mu_{bf}^2}$, is the Reynolds number; k_{bf} is the base fluid thermal conductivity; and $r_p = \left(\frac{\phi_1 r_1^3 + \phi_2 r_2^3}{\phi_1 + \phi_2}\right)^{1/3}$.

The proposed relation (eq 14) is a function of temperature, individual particle volume fraction, thermal conductivity and size, and base fluid thermal conductivity. The test data are compared with the proposed relation (eq 14) and other relations of Eid and Nafe[56] (model 5) based on the superposition for the thermal conductivity of hybrid nanofluids. The comparison is depicted in Figure 9. The

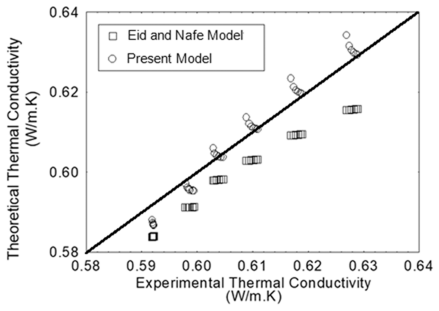

Figure 9. Comparison of the measured thermal conductivity of TiO_2−Al_2O_3/water hybrid nanofluids and estimates using the superposition model of Eid and Nafe[54] and the present model.

comparison of test data with the empirical relation (eq 14) indicates a 0.3% deviation. Hence, the empirical relation (eq 14) containing the effective thermal conductivity of nanoparticles along with an effective nanoparticle size is useful in estimating the thermal conductivity of TiO_2−Al_2O_3/water hybrid nanofluids.

5. CONCLUSIONS

Heat conduction depends on thermal conductivity. Heat transfer fluids in heat exchangers suffer from low thermal conductivity. To improve thermal conductivity, nanoparticles are mixed with base fluids. Empirical relations for the thermal conductivity of nanofluids rely on the determination of constants through the fitting of the test data. Such relations have limitations due to unjustified assumptions. This paper proposes a modified Corcione empirical relation and demonstrated its applicability with the thermal conductivity of developed TiO_2−Al_2O_3/water hybrid nanofluids. Using the modified Taguchi method, optimal process parameters are obtained for maximum thermal conductivity. Test data revealed that alumina nanofluids have maximum thermal conductivity. An enhancement of 2.4 and 2.1% was observed in the thermal conductivity of alumina (5:0) and titania (0:5) nanofluids, respectively. The thermal conductivity of titania nanoparticles is low compared to that of alumina nanoparticles. Hence, the conductivity of the hybrid solution falls above that of titania nanofluids and below that of alumina nanofluids. The thermal conductivity of hybrid nanofluids depends on the thermal conductivity of nanoparticles and the base fluid, individual particle volume fraction and size, and temperature. Thus, the developed empirical relation provides an accurate thermal conductivity of TiO_2−Al_2O_3/water hybrid nanofluids. This relation estimates the thermal conductivity of binary or

https://doi.org/10.1021/acsomega.2c07513
ACS Omega 2023, 8, 24176−24184

mono-nanofluids. Future research is directed toward the determination of the optimal particle size and performing different stability tests to achieve a high thermal conductivity for hybrid nanofluids.

AUTHOR INFORMATION

Corresponding Author

Ashok M. Sajjan − *Centre of Excellence in Material Science and Department of Chemistry, KLE Technological University, Hubballi 580031, India;* orcid.org/0000-0003-1251-8803; Phone: +91-944-8801139; Email: am_sajjan@kletech.ac.in; Fax: +91-836-2374985

Authors

Atul Bhattad − *Department of Mechanical Engineering, Koneru Lakshmaiah Education Foundation, Guntur 522502, India*

B. Nageswara Rao − *Department of Mechanical Engineering, Koneru Lakshmaiah Education Foundation, Guntur 522502, India*

Vinay Atgur − *Department of Mechanical Engineering, Koneru Lakshmaiah Education Foundation, Guntur 522502, India*

Nagaraj R. Banapurmath − *Department of Mechanical Engineering, KLE Technological University, Hubballi 580031, India; Centre of Excellence in Material Science, KLE Technological University, Hubballi 580031, India*

Chandramouli Vadlamudi − *Aerospace Integration Engineer, Aerosapien Technologies, Daytona Beach, Florida 32114, United States*

Sanjay Krishnappa − *Aerospace Integration Engineer, Aerosapien Technologies, Daytona Beach, Florida 32114, United States*

T. M. Yunus Khan − *Department of Mechanical Engineering, College of Engineering, King Khalid University, Abha 61421, Saudi Arabia;* orcid.org/0000-0002-9242-7591

Narasimha H. Ayachit − *Centre of Excellence in Material Science, KLE Technological University, Hubballi 580031, India*

Complete contact information is available at: https://pubs.acs.org/10.1021/acsomega.2c07513

Author Contributions

Conceptualization: V.A., A.B., and N.R.B.; methodology: B.N.R. and V.A.; software: V.A. and B.N.R.; validation: V.A., N.R.B., and B.N.R.; formal analysis: V.A., N.R.B., A.B., and N.H.A.; investigation: V.A and A.B.; resources: C.V., S.K., and T.M.Y.; data curation: V.A. and A.B.; writing—original draft preparation: V.A. and B.N.R.; writing—review and editing: V.A., N.R.B., A.M.S., and N.H.A.; visualization: A.M.S., C.V., and S.K.; supervision: B.N.R. and V.A.; project administration: T.M.Y., C.V., and S.K.; and funding acquisition: T.M.Y., C.V., and S.K.

Funding

This work was funded by King Khalid University under grant number (R.G.P. 2/76/44).

Notes

The authors declare no competing financial interest.

ACKNOWLEDGMENTS

The authors extend their appreciation to the Deanship of Scientific Research at King Khalid University for funding this work through a large group research project under grant number (R.G.P. 2/76/44).

REFERENCES

(1) Das, P. K. A review based on the effect and mechanism of thermal conductivity of normal nanofluids and hybrid nanofluids. *J. Mol. Liq.* **2017**, *240*, 420−446.

(2) Azmi, W. H.; Sharma, K. V.; Mamat, R.; Najafi, G.; Mohamad, M. S. The enhancement of effective thermal conductivity and effective dynamic viscosity of nanofluids-a review. *Renewable Sustainable Energy Rev.* **2016**, *53*, 1046−1058.

(3) Chen, T.; Kim, J.; Cho, H. Theoretical analysis of the thermal performance of a plate heat exchanger at various chevron angles using lithium bromide solution with nanofluid. *Int. J. Refrig.* **2014**, *48*, 233−244.

(4) Buschmann, M. H.; Franzke, U. Improvement of thermosyphon performance by employing nanofluid. *Int. J. Refrig.* **2014**, *40*, 416−428.

(5) Sözen, A.; Ozbas, E.; Menlik, T.; Cakır, M. T.; Guru, M.; Boran, K. Improving the thermal performance of diffusion absorption refrigeration system with alumina nanofluids: an experimental study. *Int. J. Refrig.* **2014**, *44*, 73−80.

(6) Khan, J. A.; Mustafa, M.; Hayat, T.; Farooq, M.; Alsaedi, A.; Liao, S. J. On model for three-dimensional flow of nanofluid: an application to solar energy. *J. Mol. Liq.* **2014**, *194*, 41−47.

(7) Das, S. K.; Putra, N.; Thiesen, P.; Roetzel, W. Temperature dependence of thermal conductivity enhancement for nanofluids. *J. Heat Transfer* **2003**, *125*, 567−574.

(8) Timofeeva, E. V.; Gavrilov, A. N.; McCloskey, J. M.; Tolmachev, Y. V.; et al. Thermal conductivity and particle agglomeration in alumina nanofluids: experiment and theory. *Phys. Rev. E* **2007**, *76*, No. 061203.

(9) Oh, D-W.; Jain, A.; Eaton, J. K.; Goodson, K. E.; Lee, J. S. Thermal conductivity measurement and sedimentation detection of aluminium oxide nanofluids by using the 3ω method. *Int. J. Heat Fluid Flow.* **2008**, *29*, 1456−1461.

(10) Berger Bioucas, F. E.; Rausch, M. H.; Schmidt, J.; Bück, A.; Koller, T. M.; Fröba, A. P. Effective thermal conductivity of nanofluids: measurement and prediction. *Int. J. Thermophys.* **2020**, *41*, 55.

(11) Gonçalves, I.; Souza, R.; Coutinho, G.; Miranda, J.; Moita, A.; Pereira, J. E.; Moreira, A.; Lima, R. Thermal conductivity of nanofluids: a review on prediction models, controversies and challenges. *Appl. Sci.* **2021**, *11*, 2525.

(12) Zendehboudi, A.; Saidur, R. A reliable model to estimate the effective thermal conductivity of nanofluids. *Heat Mass Transfer* **2019**, *55*, 397−411.

(13) Kaplan, M.; Çarpınlıoğlu, M.Ö. Proposed new equations for calculation of thermophysical properties of nanofluids. *Int. Adv. Res. Eng. J.* **2021**, *5*, 142−151.

(14) Sarkar, J.; Ghosh, P.; Adil, A. A review on hybrid nanofluids: Recent research, development, and applications. *Renewable Sustainable Energy Rev.* **2015**, *43*, 164−177.

(15) Gupta, M.; Singh, V.; Kumar, S.; Kumar, S.; Dilbaghi, N.; Said, Z. Up to date review on the synthesis and thermophysical properties of hybrid nanofluids. *J. Cleaner Prod.* **2018**, *190*, 169−192.

(16) Sundar, L. S.; Sharma, K. V.; Singh, M. K.; Sousa, A.C.M. Hybrid nanofluids preparation, thermal properties, heat transfer and friction factor − A review. *Renewable Sustainable Energy Rev.* **2017**, *68*, 185−198.

(17) Qi, C.; Wan, Y. L.; Wang, G. Q.; Han, D. T. Study on stabilities, thermophysical properties and natural convective heat transfer characteristics of TiO_2-water nanofluids. *Indian J. Phys.* **2018**, *92*, 461−478.

(18) Das, P. K.; Mallik, A. K.; Ganguly, R.; Santra, A. K. Synthesis and characterization of TiO_2-water nanofluids with different surfactants. *Int. Commun. Heat Mass Transfer* **2016**, *75*, 341−348.

(19) Alkasmoul, F. S.; Al-Asadi, M. T.; Myers, T. G.; Thompson, H. M.; Wilson, M.C.T. A practical evaluation of the performance of

https://doi.org/10.1021/acsomega.2c07513
ACS Omega 2023, 8, 24176−24184

Al_2O_3-water, TiO_2-water and CuO-water nanofluids for convective cooling. *Int. J. Heat Mass Transfer* **2018**, *126*, 639−651.
(20) Khaleduzzaman, S. S.; Saidur, R.; Mahbubul, I. M.; Ward, T. A.; Sohel, M. R.; Shahrul, I. M.; Selvaraj, J.; Rahman, M. M. Energy, exergy, and friction factor analysis of nanofluid as a coolant for electronics. *Ind. Eng. Chem. Res.* **2014**, *53*, 10512−10518.
(21) Senthilkumar, A. P.; Karthikeyan, P.; Janaki, S.; Reddy, E. P.; Rahman, Z. W.; Raajasimman, G. Effectiveness study on Al_2O_3-TiO_2 nanofluid heat exchanger. *Int. J. Eng. Robot Technol.* **2016**, *3*, 73−81.
(22) Maddah, H.; Aghayari, R.; Mirzaee, M.; Hossein, M.; et al. Factorial experimental design for the thermal performance of a double pipe heat exchanger using Al_2O_3-TiO_2 hybrid nanofluid. *Int. Commun. Heat Mass Transfer* **2018**, *97*, 92−102.
(23) Hamid, K. A.; Azmi, W. H.; Nabil, M. F.; Mamat, R.; Sharma, K. V. Experimental investigation of thermal conductivity and dynamic viscosity on nanoparticle mixture ratios of TiO_2-SiO_2 nanofluids. *Int. J. Heat Mass Transfer* **2018**, *116*, 1143−1152.
(24) Hamid, K. A.; Azmi, W. H.; Nabil, M. F.; Mamat, R. Experimental investigation of nanoparticle mixture ratios on TiO_2−SiO_2 nanofluids heat transfer performance under turbulent flow. *Int. J. Heat Mass Transfer* **2018**, *118*, 617−627.
(25) Charab, A. A.; Movahedirad, S.; Norouzbeigi, R. Thermal conductivity of Al_2O_3+TiO_2/water nanofluid: Model development and experimental validation. *Appl. Therm. Eng.* **2017**, *119*, 42−51.
(26) Chougule, S. S.; Sahu, S. K. *Model of Heat Conduction In Hybrid Nanofluid*, IEEE Int. Conf. Emerg. Trends Comput. Commun. Nanotechnology, ICE-CCN, 2013; pp 337−341.
(27) Takabi, B.; Salehi, S. Augmentation of the heat transfer performance of a sinusoidal corrugated enclosure by employing hybrid nanofluid. *Adv. Mech. Eng.* **2014**, *6*, 147059.
(28) Hemmat Esfe, M.; Arani, A.A.A.; Rezaie, M.; Yan, W. M.; Karimipour, A. Experimental determination of thermal conductivity and dynamic viscosity of Ag-MgO/water hybrid nanofluid. *Int. Commun. Heat Mass Transfer.* **2015**, *66*, 189−195.
(29) Hemmat Esfe, M.; Saedodin, S.; Biglari, M.; Rostamian, H. Experimental investigation of thermal conductivity of CNTs-Al_2O_3/water: A statistical approach. *Int. Commun. Heat Mass Transfer.* **2015**, *69*, 29−33.
(30) Zadkhast, M.; Toghraie, D.; Karimipour, A. Developing a new correlation to estimate the thermal conductivity of MWCNT-CuO/water hybrid nanofluid via an experimental investigation. *J. Therm. Anal. Calorim.* **2017**, *129*, 859−867.
(31) Esfahani, N. N.; Toghraie, D.; Afrand, M. A new correlation for predicting the thermal conductivity of ZnO−Ag (50%−50%)/water hybrid nanofluid: An experimental study. *Powder Technol.* **2018**, *323*, 367−373.
(32) Das, N. K.; Naik, P. K.; Reddy, D. N.; Mallik, B. S.; Bose, S.; Banerjee, T. Experimental and molecular dynamic insights on the thermophysical properties for MWCNT-Phosphonium based eutectic thermal media. *J. Mol. Liq.* **2022**, *354*, No. 118892.
(33) Singh, S. K. Review on the stability of the nanofluids. In *Pipeline Engineering*; Rushd, S.; Ismail, M. A., Eds.; IntechOpen, 2022.
(34) Safiei, W.; Rahman, M. M.; Yusoff, A. R.; Radin, M. R. Preparation, stability and wettability of nanofluid: A review. *J. Mech. Eng. Sci.* **2020**, *14*, 7244−7257.
(35) Amin, A.-T.; Hamzah, W.A.W.; Oumer, A. N. Thermal conductivity and dynamic viscosity of mono and hybrid organic- and synthetic-based nanofluids: A critical review. *Nanotechnol. Rev.* **2021**, *10*, 1624−1661.
(36) Malika, M.; Sonawane, S. S. Effect of nanoparticle mixed ratio on stability and thermo-physical properties of CuO-ZnO/water-based hybrid nanofluid. *J. Indian Chem. Soc.* **2020**, *97*, 414−419.
(37) Sahoo, R. R.; Kumar, V. Comparative analysis of Viscosity and Thermal Conductivity for Al_2O_3/CuO Hybrid Nanofluid in Binary Base Fluids. *Nanotechnol. Mater. Sci.* **2019**, *6*, 34−42.
(38) Ramadhan, A. I.; Azmi, W. H.; Mamat, R.; Hamid, K. A.; Norsakinah, S. Investigation on stability of *tri*-hybrid nanofluids in water- ethylene glycol mixture. *IOP Conf. Ser.: Mater. Sci. Eng.* **2018**, *469*, No. 012068.
(39) Wciślik, S. Efficient stabilization of mono and hybrid nanofluids. *Energies* **2020**, *13*, 3793.
(40) Afshari, F.; Manay, E.; Rahimpour, S.; Sahin, B.; Muratçobanoglu, B.; Teimuri-Mofrad, R. A review study on factors affecting the stability of nanofluids. *Heat Transfer Res.* **2022**, *53*, 77−91.
(41) Arora, N.; Gupta, M. *Stability Evaluation and Enhancement Methods in Nanofluids: A Review*, AIP Conference Proceedings, 2021; p 040022.
(42) Zainon, S. N. M.; Azmi, W. H. Recent Progress on Stability and Thermo-Physical Properties of Mono and Hybrid towards Green Nanofluids. *Micromachines* **2021**, *12*, 176.
(43) Bumataria, R. K.; Chavda, N. K.; Panchal, H. Current research aspects in mono and hybrid nanofluid based heat pipe technologies. *Heliyon* **2019**, *5*, No. e01627.
(44) Ali, A. R. I.; Salam, B. A review on nanofluid: preparation, stability, thermophysical properties, heat transfer characteristics and application. *SN Appl. Sci.* **2020**, *2*, 1636.
(45) Bhattad, A.; Rao, B. N.; Atgur, V.; Veza, I.; Zamri, M.F.M.A.; Fattah, I.M.R. Thermal performance evaluation of plate-type heat exchanger with alumina-titania hybrid suspensions. *Fluids.* **2023**, *8*, 120.
(46) Xu, Q.; Liu, L.; Feng, J.; Qiao, L.; Yu, C.; Shi, W.; et al. A comparative investigation on the effect of different nanofluids on the thermal performance of two-phase closed thermosyphon. *Int. J. Heat Mass Transf.* **2020**, *149*, No. 119189.
(47) Ross, P. J. *Taguchi Techniques for Quality Engineering*; McGraw-Hill: Singapore, 1989.
(48) Rajyalakshmi, K.; Boggarapu, N. R. Expected range of the output response for the optimum input parameters utilizing the modified Taguchi approach. *Multidiscip. Model. Mater. Struct.* **2019**, *15*, 508−522.
(49) Koneru, S.; Srinath, A.; Rao, B. N. Multiobjective optimization for the optimal heat pipe working parameters based on Taguchi's design of experiments. *Heat Transfer* **2021**, *51*, 2510−2523.
(50) Mallesh, M. B.; Banapurmath, N. R.; Manzoore Elahi, M. S.; Vinay, A.; Nazia, H.; Mujtaba, M. A.; Yunus Khan, T. M.; Nageswara Rao, B.; Khadiga, A. I.; Ashraf, E. Performance indicators for the optimal BTE of biodiesels with additives through engine testing by the Taguchi approach. *Chemosphere.* **2022**, *288*, No. 132450.
(51) Dharmendra, B. V.; Kodali, S. P.; Rao, B. N. A simple and reliable Taguchi approach for multi-objective optimization to identify optimal process parameters in nano-powder-mixed electrical discharge machining of INCONEL800 with copper electrode. *Heliyon* **2019**, *5*, e02326.
(52) Khanafer, K.; Vafai, K. A critical synthesis of thermo physical characteristics of nanofluids. *Int. J. Heat Mass Transfer.* **2011**, *54*, 4410−4428.
(53) Xuan, Y.; Li, Q.; Hu, W. Aggregation structure and thermal conductivity of nanofluids. *AIChE J.* **2003**, *49*, 1038−1043.
(54) Corcione, M. Empirical correlating equations for predicting the effective thermal conductivity and dynamic viscosity of nanofluids. *Energy Convers. Manage.* **2011**, *52*, 789−793.
(55) Tiwari, A. K.; Pradyumna, G.; Jahar, S. Investigation of thermal conductivity and viscosity of nanofluid. *J. Environ Res. Develop.* **2012**, *7*, 768−777.
(56) Eid, M. R.; Nafe, M. A. Thermal conductivity variation and heat generation effects on magneto-hybrid nanofluid flow in a porous medium with slip condition. *Waves Random Complex Media* **2022**, *32*, 1103−1127.

https://doi.org/10.1021/acsomega.2c07513
ACS Omega 2023, 8, 24176−24184